INTO THE WILD WITH AUDIOSCOPE: UNSUPERVISED AUDIO-VISUAL SEPARATION OF ON-SCREEN SOUNDS

Anonymous authors
Paper under double-blind review

ABSTRACT

Recent progress in deep learning has enabled many advances in sound separation and visual scene understanding. However, extracting sound sources which are apparent in natural videos remains an open problem. In this work, we present *AudioScope*, a novel audio-visual sound separation framework that can be trained without supervision to isolate on-screen sound sources from real in-the-wild videos. Prior audio-visual separation work assumed artificial limitations on the domain of sound classes (e.g., to speech or music), constrained the number of sources, and required strong sound separation or visual segmentation labels. AudioScope overcomes these limitations, operating on an open domain of sounds, with variable numbers of sources, and without labels or prior visual segmentation. The training procedure for AudioScope uses mixture invariant training (MixIT) to separate synthetic mixtures of mixtures (MoMs) into individual sources, where noisy labels for mixtures are provided by an unsupervised audio-visual coincidence model. Using the noisy labels, along with attention between video and audio features, AudioScope learns to identify audio-visual similarity and to suppress off-screen sounds. We demonstrate the effectiveness of our approach using a dataset of video clips extracted from open-domain YFCC100m video data. This dataset contains a wide diversity of sound classes recorded in unconstrained conditions, making the application of previous methods unsuitable. For evaluation and semi-supervised experiments, we collected human labels for presence of on-screen and off-screen sounds on a small subset of clips.

1 INTRODUCTION

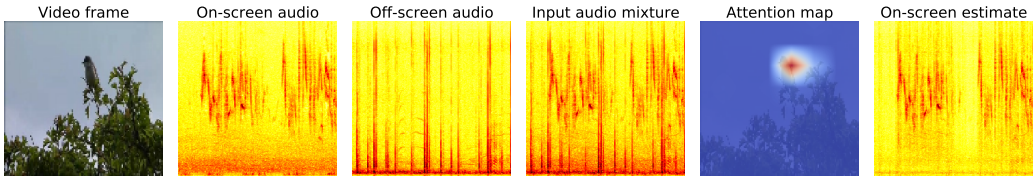

Figure 1: AudioScope separating on-screen bird chirping from wind noise and off-screen sounds from fireworks and human laugh.

Audio-visual machine perception has been undergoing a renaissance in recent years driven by advances in large-scale deep learning. A motivating observation is the interplay in human perception between auditory and visual perception. We understand the world by parsing it into the objects that are the sources of the audio and visual signals we can perceive. However, the sounds and sights produced by these sources have rather different and complementary properties. Objects may make sounds intermittently, whereas their visual appearance is typically persistent. The visual percepts of different objects tend to be spatially distinct, whereas sounds from different sources can blend together and overlap in a single signal, making it difficult to separately perceive the individual sources. This suggests that there is something to be gained by aligning our audio and visual percepts: if we can identify which audio signals correspond to which visual objects, we can selectively attend to an object's audio signal by visually selecting the object.

This intuition motivates using vision as an interface for audio processing, where a primary problem is to selectively preserve desired sounds, while removing unwanted sounds. In some tasks, such as speech enhancement, the desired sounds can be selected by their class: speech versus non-speech in this case. In an open-domain setting, the selection of desired sounds is at the user's discretion. This presents a user-interface problem: it is challenging to select sources in an efficient way using audio. This problem can be greatly simplified in the audio-visual case if we use video selection as a proxy for audio selection, for example, by selecting sounds from on-screen objects, and removing off-screen sounds. Recent work has used video for selection and separation of speech (Ephrat et al., 2018; Afouras et al., 2020) or music (Zhao et al., 2018; Gao & Grauman, 2019; Gan et al., 2020). However, systems that address this for arbitrary sounds (Gao et al., 2018; Rouditchenko et al., 2019; Owens & Efros, 2018) may be useful in more general cases, such as video recording, where the sounds of interest cannot be defined in advance.

The problem of associating arbitrary sounds with their visual objects is challenging in an open domain. Several complications arise that have not been fully addressed by previous work. First, a large amount of training data is needed in order to cover the space of possible sound. Supervised methods require labeled examples where isolated on-screen sounds are known. The resulting data collection and labeling burden limits the amount and quality of available data. To overcome this, we propose an unsupervised approach using mixture invariant training (MixIT) (Wisdom et al., 2020b), that can learn to separate individual sources from in-the-wild videos, where the on-screen and off-screen sounds are unknown. Another problem is that different audio sources may correspond to a dynamic set of on-screen objects in arbitrary spatial locations. We accommodate this by using attention mechanisms that align each hypothesized audio source with the different spatial and temporal positions of the corresponding objects in the video. Finally we need to determine which audio sources appear on screen, in the absence of strong labels. This is handled using a weakly trained classifier for sources based on audio and video embeddings produced by the attention mechanism.

2 Relation to previous work

Separation of arbitrary sounds from a mixture, known as "universal sound separation," was recently shown to be possible with a fixed number of sounds (Kavalerov et al., 2019). Conditional information about which sound classes are present can improve separation performance (Tzinis et al., 2020). The FUSS dataset (Wisdom et al., 2020a) expanded the scope to separate a variable number of sounds, in order to handle more realistic data. A framework has also been proposed where specific sound classes can be extracted from input sound mixtures (Ochiai et al., 2020). These approaches require curated data containing isolated sounds for training, which prevents their application to truly open-domain data and introduces difficulties such as annotation cost, accurate simulation of realistic acoustic mixtures, and biased datasets.

To avoid these issues, a number of recent works have proposed replacing the strong supervision of reference source signals with weak supervision labels from related modalities such as sound class (Pishdadian et al., 2019; Kong et al., 2020), visual input (Gao & Grauman, 2019), or spatial location from multi-microphone recordings (Tzinis et al., 2019; Seetharaman et al., 2019; Drude et al., 2019). Most recently, Wisdom et al. (2020b) proposed mixture invariant training (MixIT), which provides a purely unsupervised source separation framework for a variable number of latent sources.

A variety of research has laid the groundwork towards solving audio-visual on-screen source separation (Michelsanti et al., 2020). Generally, the two main approaches are to use audio-visual localization (Hershey & Movellan, 2000; Senocak et al., 2018; Wu et al., 2019; Afouras et al., 2020), or object detection networks, either supervised (Ephrat et al., 2018; Gao & Grauman, 2019; Gan et al., 2020) or unsupervised (Zhao et al., 2018), to predict visual conditioning information. However, these works only consider restricted domains such as speech (Hershey & Casey, 2002; Ephrat et al., 2018; Afouras et al., 2020) or music (Zhao et al., 2018; Gao & Grauman, 2019; Gan et al., 2020). Gao et al. (2018) reported results with videos from a wide domain, but relied on supervised visual object detectors, which precludes learning about the appearance of sound sources outside of a closed set of classes defined by the detectors. Rouditchenko et al. (2019) proposed a system for a wide domain of sounds, but required sound class labels as well as isolated sounds from these classes. Our approach avoids the supervision of class labels and isolated sources in order to handle unknown visual and sound classes occurring in multi-source data.

Towards learning directly from a less restrictive open domain of in-the-wild video data, Tian et al. (2018) learn to localize audio-visual events in unconstrained videos and present an ad hoc dataset (Korbar et al., 2018) that pre-trains models to discern temporal synchronization of audio-video pairs, and demonstrate promising results on action recognition and audio classification. Arandjelovic & Zisserman (2017) take a similar approach by classifying audio-visual correspondences of pairs of one video frame and one second of audio. Hu et al. (2020) proposed a curriculum learning approach where the model gradually learns harder examples to separate.

Closest to our work is the approach of Owens & Efros (2018), a self-supervised audio-visual on-screen speech separation system based on temporal audio-visual alignment. However, Owens & Efros (2018) makes the restrictive assumptions of a fixed number of speakers and training videos containing only on-screen sources.

Our approach significantly differs from these prior works in that we do not restrict our domain to musical instruments or human speakers, and we train and test with real in-the-wild videos containing an arbitrary number of objects with no object class restrictions. Our proposed framework can deal with noisy labels (e.g. videos with no on-screen sounds), operate on a completely open-domain of in-the-wild videos, and effectively isolate sounds coming from on-screen objects.

We address the following task, which extends the formulation of the on-screen speech separation problem (Owens & Efros, 2018). Given any input video, the goal is to separate all sources that constitute the input mixture, and then estimate an audio-visual correspondence score for each separated source. These probability scores should be high for separated sources which are apparent on-screen, and low otherwise. The separated audio sources, weighted by their estimated on-screen probabilities, can be summed together to reconstruct the on-screen mixture. We emphasize that our approach is more generally applicable than previous proposals, because real-world videos can contain an unknown number of both on-screen and off-screen sources belonging to an undefined ontology of classes.

We make the following contributions in this paper:

1. We provide the first solution for training an unsupervised, open-domain, audio-visual on-screen separation system from scratch on real in-the-wild video data, with no requirement on modules such as object detectors that require supervised data.
2. We provide a new dataset for the on-screen audio-visual separation task, consisting of $2{,}500$ hours of unlabeled videos from YFCC100m, and 55 hours of videos that are human-labeled for presence of on-screen and off-screen sounds.

3 Model architecture

The overall architecture of AudioScope is depicted in Figure 2.

3.1 Audio separation network

The separation network architecture consists of learnable convolutional encoder and decoder layers with an improved time-domain convolutional network (TDCN++) masking network (Wisdom et al., 2020b). A mixture consistency projection (Wisdom et al., 2019) is applied to constrain separated sources to add up to the input mixture. The separation network processes a T-sample input mixture waveform and outputs M estimated sources $\hat{\mathbf{s}} \in \mathbb{R}^{M \times T}$. The masking network estimates M masks which are multiplied with the activations of the encoded input mixture. The final time-domain signals $\hat{\mathbf{s}}$ are computed by applying the decoder, a transposed convolutional layer, to the masked coefficients.

3.2 Audio embedding network

For each separated source $\hat{s}_m$, we extract a corresponding global audio embedding use the MobileNet v1 architecture (Howard et al., 2017), consisting of stacked 2D separable dilated convolutional blocks with a dense layer at the end. The network first computes log Mel-scale spectrograms with F_{a} audio frames from the time-domain separated sources, and then applies stacks of depthwise separable convolutions to produce the $F_{\mathrm{a}} \times N$ embedding matrix $\mathcal{M}_m^{\mathrm{a}}$, which contains an N-dimensional

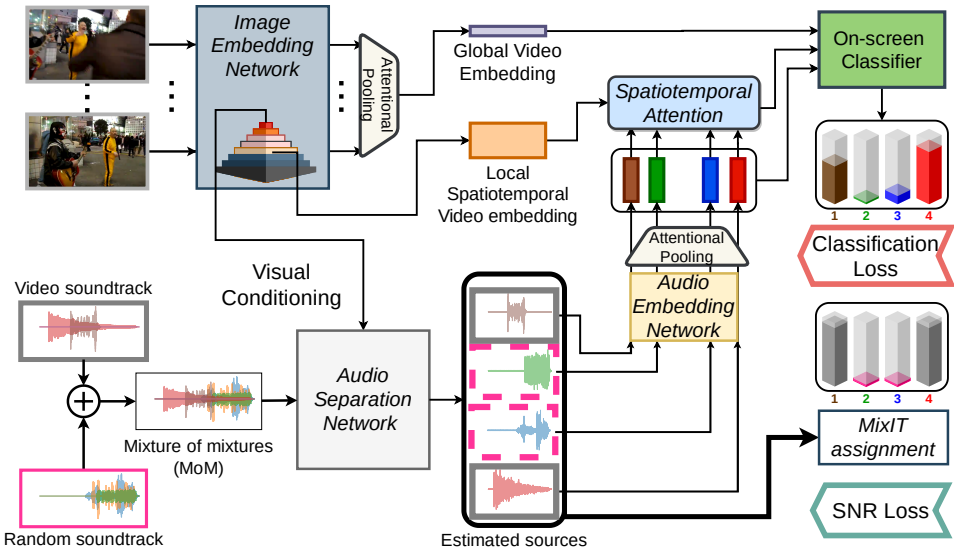

Figure 2: AudioScope system diagram with 2 input mixtures and 4 output sources.

row embedding for each frame. An attentional pooling operation (Girdhar & Ramanan, 2017) is used, for each source, m, to form an embedding vector $Z_m = \text{attend}(\bar{\mathcal{M}}^{\text{a}}_m, \mathcal{M}^{\text{a}}_m, \mathcal{M}^{\text{a}}_m)$, where the average embedding $\bar{\mathcal{M}}^{\text{a}}_m = \frac{1}{F_{\text{a}}} \sum_i \mathcal{M}^{\text{a}}_{m,i}$ is the query vector for source m. The attention mechanism (Bahdanau et al., 2014) is defined as

$$\text{attend}(q, K, V) = \alpha^T f_{\text{V}}(V), \quad \alpha = \text{softmax}(f_{\text{K}}(K) f_{\text{q}}(q)^T), \tag{1}$$

with query row vector q, the attention weight distribution column vector α, key matrix K, value matrix V, and trainable row-wise dense layers f_{q}, f_{V}, f_{K}, all having conforming dimensions.

3.3 Image embedding network

To extract visual features from video frames, we again use a MobileNet v1 architecture. This visual embedding model $\mathcal{M}^{\text{v}}$ is applied independently to each one of the F_{v} input video frames and a static-length embedding is extracted for each image $\mathcal{M}^{\text{v}}_j, \;\; j \in \{1, \ldots, F_{\text{v}}\}$.

Conditioning separation network with the temporal video embedding: The embeddings of the video input $\mathcal{M}^{\text{v}}_j$ can be used to condition the separation network, following the same procedure as Tzinis et al. (2020). The concatenated visual embedding is resampled, fed through a dense layer, and concatenated together with all convolutional blocks.

Global video embedding: A global embedding of the video input is extracted using attentional pooling over all video frames, given by $V^{\text{g}} = \text{attend}(\bar{\mathcal{M}}^{\text{v}}, \mathcal{M}^{\text{v}}, \mathcal{M}^{\text{v}})$, where the average embedding $\bar{\mathcal{M}}^{\text{v}} = \frac{1}{F_{\text{v}}} \sum_j \mathcal{M}^{\text{v}}_j$ is the query vector.

Local spatio-temporal video embedding: We also use local features extracted from an intermediate level in the visual convolutional network, that has 8×8 spatial locations. These are denoted $\mathcal{M}^{\text{vl}}_k$, where $k = (j, n)$ indexes video frame j and spatial location index n. These provide spatial features for identification of sources with visual objects to be used with audio-visual spatio-temporal attention.

3.4 Audio-visual spatio-temporal attention

An important aspect of this work is to combine audio and visual information in order to infer correspondence between each separated source and the relevant objects in video. This in turn will be used to identify which sources are visible on-screen. To this end, we employ an audio-visual spatio-temporal attention scheme by letting the network attend to the local features of the visual embeddings for each separated source. In this mechanism, we use the global audio embedding Z_m as the query input for source m, and the key and value inputs are given by the spatio-temporal video embeddings, $\mathcal{M}^{\text{vl}}$, so that the video embedding extracted by source m is $R_m = \text{attend}(Z_m, \mathcal{M}^{\text{vl}}, \mathcal{M}^{\text{vl}})$.

3.5 ON-SCREEN CLASSIFIER

To infer the visual presence each separated source, we concatenate the global video embedding V^{g}, the global audio embedding for each source Z_m, and the corresponding local spatio-temporal audio-visual embedding R_m. The concatenated vector is fed through a dense layer with a logistic activation: $\hat{y}_m = \text{logistic}\left([V^{\mathrm{g}}, Z_m, R_m]\right)$.

4 TRAINING LOSSES

4.1 SEPARATION LOSS

We use a MixIT separation loss (Wisdom et al., 2020b), which optimizes the assignment of M estimated sources $\hat{\mathbf{s}} = \mathcal{M}_s\left(x_1 + x_2\right)$ to two reference mixtures x_1, x_2 as follows:

$$\mathcal{L}_{\text{sep}}\left(x_1, x_2, \hat{\mathbf{s}}\right) = \min_{\mathbf{A}} \Big(\mathcal{L}_{\text{SNR}}\left(x_1, [\mathbf{A}\hat{\mathbf{s}}]_1\right) + \mathcal{L}_{\text{SNR}}\left(x_2, [\mathbf{A}\hat{\mathbf{s}}]_2\right) \Big), \tag{2}$$

where the mixing matrix $\mathbf{A} \in \mathbb{B}^{2\times M}$ is constrained to the set of $2 \times M$ binary matrices where each column sums to 1 and the SNR loss is defined as

$$\mathcal{L}_{\text{SNR}}(y, \hat{y}) = 10 \log_{10}\left(\|y - \hat{y}\|^2 + 10^{-3}\|y\|^2\right). \tag{3}$$

Due to the constraints on $\mathbf{A}$, each source $\hat{s}_i$ can only be assigned to one reference mixture.

4.2 CLASSIFICATION LOSS

To train the on-screen classifier, we consider the following classification losses.

Exact binary cross entropy: The following loss function uses a binary label y_m for each source m, which in the unsupervised case is given by the MixIT assignment.

$$\mathcal{L}_{\text{exact}} = \sum_{m=1}^{M} \Big(-y_m \log\left(\hat{y}_m\right) + \left(y_m - 1\right) \log\left(1 - \hat{y}_m\right) \Big). \tag{4}$$

Multiple-instance cross entropy: Since some separated sources assigned to the on-screen mixture are not on-screen, a multiple-instance (MI) (Maron & Lozano-Pérez, 1998) loss, which minimizes over the set of positive labels $\mathcal{R} = \{m | y_m = 1, \;\; m \in \{1, \ldots, M\}\}$ may be more robust:

$$\mathcal{L}_{\text{MI}} = \min_{m \in \mathcal{R}} \Big(-\log\left(\hat{y}_m\right) - \sum_{m' \notin \mathcal{R}} \log\left(1 - \hat{y}_{m'}\right) \Big). \tag{5}$$

Active combinations cross entropy: An alternative to the MI loss, *active combinations* (AC), corresponds to the minimum loss over all settings $\wp_{\geq 1}\left(\mathcal{R}\right)$ of the labels such that at least one label is positive:

$$\mathcal{L}_{\text{AC}} = \min_{\mathcal{A} \in \wp_{\geq 1}(\mathcal{R})} \Big(-\sum_{m \in \mathcal{A}} \log\left(\hat{y}_m\right) - \sum_{m' \notin \mathcal{A}} \log\left(1 - \hat{y}_{m'}\right) \Big). \tag{6}$$

5 EXPERIMENTAL FRAMEWORK

5.1 DATA PREPARATION

In order to train on real-world audio-visual recording environments for our open-domain system, we use the Yahoo Flickr Creative Commons 100 Million Dataset (YFCC100m) (Thomee et al., 2016). The dataset consists of about 200,000 videos (2,500 hours) of various lengths and covering a diverse range of semantic sound categories. We extract 5-second clips with a hop size of 1 second, resulting in around 7.2 million clips. Clips consist of a 5-second audio waveform sampled at 16 kHz and 5 video frames $x^{(f)}$, where each frame is a $128 \times 128 \times 3$ RGB image.

Our goal is to train our system completely unsupervised, but we sought to reduce the proportion of videos where there are no on-screen sounds. We thus created a filtered subset $\mathcal{D}_f$ of YFCC100m of

clips with a high audio-visual coincidence probability predicted by an unsupervised audio-visual coincidence prediction model (Jansen et al., 2020) trained on sounds from Audioset (Gemmeke et al., 2017). The resulting selection is noisy, because the coincidence model is not perfect and clips that have high audio-visual coincidence may contain both on-screen and off-screen sounds, or even no on-screen sounds, but at least improves the presence of on-screen sounds, as shown below.

The final filtered dataset consists of all clips extracted from the $36{,}000$ highest audio-visual coincidence scoring videos. The threshold for filtering was empirically set to keep a fair amount of diverse videos while ensuring that not too many clips with only *off-screen* were accepted.

In order to evaluate the performance of the unsupervised filtering as well as our proposed models, and to experiment with a small amount of supervised data, we randomly selected $20{,}000$ unfiltered video clips and $20{,}000$ filtered clips to obtain human annotations. In the annotation process, the raters chose whether on-screen or off-screen sounds are present or not present. Each clip is labeled by 3 individual raters, and a clip is only considered on-screen or off-screen only if all 3 raters are unanimous. We constructed and on-screen subset with 836 clips for training, 735 for validation, and 295 for test, and an off-screen subset with $3{,}681$ clips for training, 836 for validation, and 370 for test.

Based on human annotations, we estimate that for unfiltered data 71.3% of clips contain both on-and-off-screen sounds, 2.8% contain on-screen-only sounds, and 25.9% contain off-screen-only. For the filtered data, 83.5% of clips contain on-screen and off-screen sounds, 5.6% of clips are on-screen-only, and 10.9% are off-screen-only. Thus the unsupervised filtering significantly reduced the proportion of off-screen-only clips.

5.2 Training

Both audio and visual embedding networks were pre-trained on Audioset (Gemmeke et al., 2017) for unsupervised coincidence prediction (Jansen et al., 2020) and fine-tuned on our data, whereas the separation network is trained from scratch using MixIT (2) on mixtures of mixtures (MoMs) constructed from the audio of our data. All models are trained on 4 Google Cloud TPUs (16 chips) with the Adam optimizer (Kingma & Ba, 2015), a batch size of 256, and learning rate of 10^{-4}.

In order to train the overall network, we use $2{,}500$ hours of unlabeled video-clips and construct minibatches of video clips with MoMs as audio. The first mixture in these MoMs is one of four types:

1. NOn: noisy-labeled on-screen.
2. SOff: synthetic off-screen-only.
3. LOn: human-labeled on-screen-only.
4. LOff: human-labeled off-screen-only.

For all example types, the second mixture in the MoM is audio drawn from a different random video in the unfiltered data. A NOn MoM uses video clip frames and audio from the filtered high-coincidence subset of our data, $\mathcal{D}_f$. SOff MoMs are constructed by combining video frames of an unfiltered clip with random audio drawn from a different unfiltered video. Unsupervised training minibatches consist of either 0% or 25% SOff examples, and the remaining examples are NOn.

Semi-supervised minibatches additionally include LOn and LOff examples, which are constructed in the manner as NOn, except that the first mixture is drawn from unanimously human-labeled on-screen-only videos and unanimously human-labeled off-scren-only videos, respectively. We experiment with using 0% or 25% SOff examples, which corresponds to minibatch (NOn, SOff, LOn, LOff) proportions of (50%, 0%, 25%, 25%) and (25%, 25%, 25%, 25%), respectively.

Classification labels y_m for all separated sources $\hat{s}_m$ in SOff and LOff examples are set to 0. For NOn and LOn examples, we set the label for each separated source as $y_m = A_{0,m}$, where $\mathbf{A}$ is the MixIT assignment matrix (2). The MixIT separation loss (2) is used for all MoM example types.

5.3 Evaluation

All evaluations use human-labeled test videos, which have been unanimously labeled as containing either only on-screen or only off-screen sounds. Using this data, we construct four evaluation sets: on-screen single mixtures, off-screen single mixtures, on-screen MoMs, and off-screen MoMs. The single mixture evaluations consist of only data drawn from the particular label, either on-screen or off-screen. Each on-screen (off-screen) MoM consists of an on-screen-only (off-screen-only) video clip, mixed with the audio from another random clip, drawn from the off-screen-only examples.

5.3.1 ON-SCREEN DETECTION

Detection performance for the on-screen classifier is measured using the area under the curve of the receiver operator characteristic (AUC-ROC). To avoid ambiguous classification decisions due to inactive or very quiet separated sources, we use a weight for each source signal's prediction equal to the linear power ratio between the powers of the source and input MoM. For single mixture evaluations, positive labels are assumed for all separated sources that are estimated from on-screen-only mixtures, and negative labels for all separated sources from off-screen-only mixtures. For on-screen MoM evaluations, labels for separated sources from on-screen MoMs are assigned using the first row of the oracle MixIT mixing matrix, classifier outputs for sources separated from off-screen MoMs are assigned negative labels.

5.3.2 SEPARATION

Since we do not have access to individual ground-truth reference sources for our in-the-wild data, we cannot evaluate the per-source separation performance. The only references we have are mixtures. Thus, we compute an estimate of the on-screen audio by combining the separated sources using classifier predictions: $\hat{x}^{\text{on}} = \sum_{m=1}^{M} p_m \hat{s}_m$. For on-screen single mixture and MoM evaluations, we measure scale-invariant SNR (SI-SNR) (Le Roux et al., 2019), between $\hat{x}^{\text{on}}$ and the reference on-screen-only mixture $x^{(on)}$. SI-SNR measures the fidelity between a target $\mathbf{y}$ and an estimate $\hat{\mathbf{y}}$ within an arbitrary scale factor in units of decibels:

$$\text{SI-SNR}(y, \hat{y}) = 10 \log_{10} \frac{\|\alpha y\|^2}{\|\alpha y - \hat{y}\|^2}, \quad \alpha = \text{argmin}_a \|ay - \hat{y}\|^2 = y^T \hat{y} / \|y\|^2. \tag{7}$$

To measure the degree to which AudioScope rejects off-screen audio, we define the off-screen suppression ratio (OSR), which is the ratio in decibels of the power of the input mixture to the power of the on-screen estimate $\hat{x}^{\text{on}}$. We only compute OSR for off-screen evaluation examples where the input mixture only contains off-screen audio. Thus, higher OSR implies greater suppression of off-screen sounds. The minimum value of OSR is 0 dB, which means that $\hat{x}^{\text{on}}$ is equal to the input mixture, which corresponds to all on-screen classifier probabilities equal to 1.

In some cases, SI-SNR and OSR can yield infinite values. For example, the estimate $\hat{y}$ may be zero, in which case SI-SNR (7) is $-\infty$ dB. This can occur when the input SNR of an on-screen mixture in a MoM is very low and none of the separated sources are assigned to it by MixIT. Conversely, if the estimate perfectly matches the target, SI-SNR can yield a value of ∞ dB, which occurs for on-screen single mixture evaluation cases when the separated sources trivially add up to the on-screen input due to mixture consistency of the separation model. For off-screen examples, OSR can also be infinite if the separation model achieves perfect off-screen suppression by predicting zero for $\hat{x}^{\text{on}}$. To avoid including these infinite values, we elect to measure median SI-SNR and OSR.

6 RESULTS

Results are shown in Table 1. Notice that there is a trade-off between preservation of on-screen sounds, as measured by SI-SNR, and suppression of off-screen sounds, as measured by OSR: higher on-screen SI-SNR on on-screen examples generally means lower OSR on off-screen examples. Different classification losses have different operating points: for MoMs, compared to using the exact cross-entropy loss, models trained with active combinations or multiple instance loss achieve lower on-screen SI-SNR, while achieving more suppression (higher OSR) of off-screen sounds. Exact cross-entropy models achieve higher AUC-ROC for single mixtures and MoMs, and achieve better reconstruction of on-screen single mixtures at the expense of less rejection of off-screen single mixtures.

Training only with the noisy labels provided by the unsupervised coincidence model (Jansen et al., 2020) achieves lower AUC-ROC compared to the semi-supervised condition that adds a small amount of human-labeled examples. Semi-supervised and unsupervised models achieve comparable on-screen SI-SNR, but semi-supervised models achieve better off-screen suppression. For example, the best on-screen SI-SNR for unsupervised and semi-supervised is 8.0 dB and 7.3 dB, respectively, while OSR is 5.3 dB and 10.7 dB. Using 25% synthetic off-screen particularly shifts the behavior of

Table 1: Evaluation results for unanimously-annotated on-screen and off-screen mixtures. Training uses unsupervised or semi-supervised examples, with either 0% or 25% synthetic off-screen (SOff) examples (Section 5.2). Cross-entropy (CE) losses include active combinations (AC), multiple instance (MI), and exact. Note that "MixIT*" indicates SI-SNR of an oracle estimate derived using MixIT with reference mixtures, and $\hat{x}^{\text{on}}$ is the on-screen estimate produced by mixing separated sources with classifier probabilities. On-screen MoMs have a median input SI-SNR of 4.4 dB.

			Single mixture				**Mixture of mixtures**			
				On: SI-SNR (dB)		**Off: OSR (dB)**		**On: SI-SNR (dB)**		**Off: OSR (dB)**
Training	**SOff**	**CE loss**	**AUC**	**MixIT***	$\hat{x}^{\text{on}}$	$\hat{x}^{\text{on}}$	**AUC**	**MixIT***	$\hat{x}^{\text{on}}$	$\hat{x}^{\text{on}}$
Unsup	0%	AC	0.58	∞	13.5	2.5	0.77	10.5	6.3	9.4
Unsup	0%	MI	0.55	∞	11.9	3.6	0.75	10.1	5.3	**10.8**
Unsup	0%	Exact	0.62	∞	36.6	0.5	**0.81**	**10.6**	**8.0**	5.3
Unsup	25%	AC	0.57	∞	12.1	**4.3**	0.76	10.5	6.4	9.3
Unsup	25%	MI	0.62	∞	13.6	4.0	0.78	9.6	6.1	9.6
Unsup	25%	Exact	**0.64**	∞	**41.0**	0.6	**0.81**	**10.6**	7.5	4.5
Semi	0%	AC	0.71	∞	14.8	6.6	**0.82**	10.4	6.1	14.1
Semi	0%	MI	0.68	∞	12.3	11.3	0.79	9.6	4.7	21.0
Semi	0%	Exact	0.73	∞	**32.8**	4.5	0.81	10.1	**7.3**	10.7
Semi	25%	AC	0.79	∞	6.7	**54.3**	0.78	10.0	3.4	**61.8**
Semi	25%	MI	0.82	∞	6.6	52.9	0.78	9.4	2.0	60.1
Semi	25%	Exact	**0.83**	∞	6.6	53.9	0.81	10.0	2.4	61.5

semi-supervised models by biasing them towards predicting lower probabilities of on-screen. This bias results in lower on-screen SI-SNR, yet very strong off-screen rejection (i.e. very large OSRs).

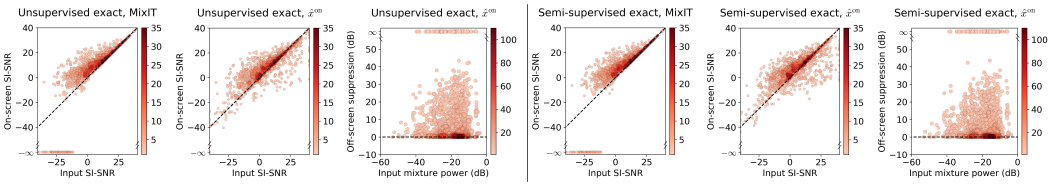

Figure 3: Scatter plots of input SI-SNR versus on-screen SI-SNR for on-screen evaluation examples, and mixture power in dB versus OSR. The settings for the models are SOff 0% and exact CE loss, and colormap indicates density of points.

Figure 3 shows scatter plots of input SI-SNR versus SI-SNR of MixIT or $\hat{x}^{\text{on}}$ on-screen estimates. From these plots, it is clear that the models tend to improve on-screen SI-SNR more often than not, and that these improvements are most significant around ± 10 dB input SI-SNR. Note that for MixIT, a number of points have a SI-SNR of $-\infty$, which happens when MixIT assigns all separated sources to the off-screen mixture. OSR is sometimes ∞ when AudioScope achieves excellent off-screen suppression, predicting nearly 0 for the on-screen audio from off-screen-only input. To provide a sense of the qualitative performance of AudioScope, we include visualizations of best, worst, and typical predictions in the appendix, and the supplementary material contains audio-visual demos.

7 Conclusion

In this paper we have proposed the first solution for training an unsupervised, open-domain, audio-visual on-screen separation system, without reliance on prior class labels or classifiers. We demonstrated the effectiveness of our system using a small amount of human-labeled, in-the-wild videos, which we also plan to release to the community. In future work, we will explore more fine-grained visual features, especially synchrony, which we expect will be especially helpful when multiple instances of the same object are present in the video. We also plan to use our trained classifier to refilter YFCC100m to get better noisy labels for the presence of on-screen sounds, which should further improve the performance of the system.

REFERENCES

Triantafyllos Afouras, Andrew Owens, Joon Son Chung, and Andrew Zisserman. Self-supervised learning of audio-visual objects from video. *arXiv preprint arXiv:2008.04237*, 2020.

Relja Arandjelovic and Andrew Zisserman. Look, listen and learn. In *Proceedings of the IEEE International Conference on Computer Vision*, pp. 609–617, 2017.

Dzmitry Bahdanau, Kyunghyun Cho, and Yoshua Bengio. Neural machine translation by jointly learning to align and translate. *arXiv preprint arXiv:1409.0473*, 2014.

Lukas Drude, Daniel Hasenklever, and Reinhold Haeb-Umbach. Unsupervised training of a deep clustering model for multichannel blind source separation. In *Proc. IEEE International Conference on Acoustics, Speech, and Signal Processing (ICASSP)*, pp. 695–699, 2019.

Ariel Ephrat, Inbar Mosseri, Oran Lang, Tali Dekel, Kevin Wilson, Avinatan Hassidim, William T Freeman, and Michael Rubinstein. Looking to listen at the cocktail party: a speaker-independent audio-visual model for speech separation. *ACM Transactions on Graphics (TOG)*, 37(4):1–11, 2018.

Chuang Gan, Deng Huang, Hang Zhao, Joshua B Tenenbaum, and Antonio Torralba. Music gesture for visual sound separation. In *Proceedings of the IEEE/CVF Conference on Computer Vision and Pattern Recognition*, pp. 10478–10487, 2020.

Ruohan Gao and Kristen Grauman. Co-separating sounds of visual objects. In *Proceedings of the IEEE International Conference on Computer Vision*, pp. 3879–3888, 2019.

Ruohan Gao, Rogerio Feris, and Kristen Grauman. Learning to separate object sounds by watching unlabeled video. In *Proceedings of the European Conference on Computer Vision (ECCV)*, pp. 35–53, 2018.

Jort F Gemmeke, Daniel P. W. Ellis, Dylan Freedman, Aren Jansen, Wade Lawrence, R Channing Moore, Manoj Plakal, and Marvin Ritter. Audio set: An ontology and human-labeled dataset for audio events. In *Proc. IEEE International Conference on Acoustics, Speech, and Signal Processing (ICASSP)*, pp. 776–780, 2017.

Rohit Girdhar and Deva Ramanan. Attentional pooling for action recognition. In *Advances in Neural Information Processing Systems*, pp. 34–45, 2017.

John R Hershey and Michael Casey. Audio-visual sound separation via hidden markov models. In *Advances in Neural Information Processing Systems*, pp. 1173–1180, 2002.

John R Hershey and Javier R Movellan. Audio vision: Using audio-visual synchrony to locate sounds. In *Advances in neural information processing systems*, pp. 813–819, 2000.

Andrew G Howard, Menglong Zhu, Bo Chen, Dmitry Kalenichenko, Weijun Wang, Tobias Weyand, Marco Andreetto, and Hartwig Adam. Mobilenets: Efficient convolutional neural networks for mobile vision applications. *arXiv preprint arXiv:1704.04861*, 2017.

Di Hu, Zheng Wang, Haoyi Xiong, Dong Wang, Feiping Nie, and Dejing Dou. Curriculum audiovisual learning. *arXiv preprint arXiv:2001.09414*, 2020.

Aren Jansen, Daniel PW Ellis, Shawn Hershey, R Channing Moore, Manoj Plakal, Ashok C Popat, and Rif A Saurous. Coincidence, categorization, and consolidation: Learning to recognize sounds with minimal supervision. In *ICASSP 2020-2020 IEEE International Conference on Acoustics, Speech and Signal Processing (ICASSP)*, pp. 121–125, 2020.

Ilya Kavalerov, Scott Wisdom, Hakan Erdogan, Brian Patton, Kevin Wilson, Jonathan Le Roux, and John R. Hershey. Universal sound separation. In *Proc. IEEE Workshop on Applications of Signal Processing to Audio and Acoustics (WASPAA)*, 2019.

Diederik P Kingma and Jimmy Ba. Adam: A method for stochastic optimization. In *Proc. International Conference on Learning Representations (ICLR)*, 2015.

Qiuqiang Kong, Yuxuan Wang, Xuchen Song, Yin Cao, Wenwu Wang, and Mark D Plumbley. Source separation with weakly labelled data: An approach to computational auditory scene analysis. In *Proc. IEEE International Conference on Acoustics, Speech, and Signal Processing (ICASSP)*, pp. 101–105, 2020.

Bruno Korbar, Du Tran, and Lorenzo Torresani. Cooperative learning of audio and video models from self-supervised synchronization. In *Advances in Neural Information Processing Systems*, pp. 7763–7774, 2018.

Jonathan Le Roux, Scott Wisdom, Hakan Erdogan, and John R. Hershey. SDR–half-baked or well done? In *Proc. IEEE International Conference on Acoustics, Speech, and Signal Processing (ICASSP)*, pp. 626–630, 2019. doi: 10.1109/icassp.2019.8683855.

Oded Maron and Tomás Lozano-Pérez. A framework for multiple-instance learning. In *Advances in neural information processing systems*, pp. 570–576, 1998.

Daniel Michelsanti, Zheng-Hua Tan, Shi-Xiong Zhang, Yong Xu, Meng Yu, Dong Yu, and Jesper Jensen. An overview of deep-learning-based audio-visual speech enhancement and separation. *arXiv preprint arXiv:2008.09586*, 2020.

Tsubasa Ochiai, Marc Delcroix, Yuma Koizumi, Hiroaki Ito, Keisuke Kinoshita, and Shoko Araki. Listen to what you want: Neural network-based universal sound selector. *arXiv preprint arXiv:2006.05712*, 2020.

Andrew Owens and Alexei A Efros. Audio-visual scene analysis with self-supervised multisensory features. In *Proceedings of the European Conference on Computer Vision (ECCV)*, pp. 631–648, 2018.

Fatemeh Pishdadian, Gordon Wichern, and Jonathan Le Roux. Finding strength in weakness: Learning to separate sounds with weak supervision. *arXiv preprint arXiv:1911.02182*, 2019.

Andrew Rouditchenko, Hang Zhao, Chuang Gan, Josh McDermott, and Antonio Torralba. Self-supervised audio-visual co-segmentation. In *ICASSP 2019-2019 IEEE International Conference on Acoustics, Speech and Signal Processing (ICASSP)*, pp. 2357–2361. IEEE, 2019.

Prem Seetharaman, Gordon Wichern, Jonathan Le Roux, and Bryan Pardo. Bootstrapping single-channel source separation via unsupervised spatial clustering on stereo mixtures. In *Proc. IEEE International Conference on Acoustics, Speech, and Signal Processing (ICASSP)*, pp. 356–360, 2019.

Arda Senocak, Tae-Hyun Oh, Junsik Kim, Ming-Hsuan Yang, and In So Kweon. Learning to localize sound source in visual scenes. In *Proceedings of the IEEE Conference on Computer Vision and Pattern Recognition*, pp. 4358–4366, 2018.

Bart Thomee, David A Shamma, Gerald Friedland, Benjamin Elizalde, Karl Ni, Douglas Poland, Damian Borth, and Li-Jia Li. Yfcc100m: The new data in multimedia research. *Communications of the ACM*, 59(2):64–73, 2016.

Yapeng Tian, Jing Shi, Bochen Li, Zhiyao Duan, and Chenliang Xu. Audio-visual event localization in unconstrained videos. In *Proceedings of the European Conference on Computer Vision (ECCV)*, pp. 247–263, 2018.

Efthymios Tzinis, Shrikant Venkataramani, and Paris Smaragdis. Unsupervised deep clustering for source separation: Direct learning from mixtures using spatial information. In *Proc. IEEE International Conference on Acoustics, Speech, and Signal Processing (ICASSP)*, pp. 81–85, 2019.

Efthymios Tzinis, Scott Wisdom, John R. Hershey, Aren Jansen, and Daniel P. W. Ellis. Improving universal sound separation using sound classification. In *Proc. IEEE International Conference on Acoustics, Speech, and Signal Processing (ICASSP)*, pp. 96–100, 2020.

Scott Wisdom, John R. Hershey, Kevin Wilson, Jeremy Thorpe, Michael Chinen, Brian Patton, and Rif A. Saurous. Differentiable consistency constraints for improved deep speech enhancement. In *Proc. IEEE International Conference on Acoustics, Speech, and Signal Processing (ICASSP)*, pp. 900–904, 2019.

Scott Wisdom, Hakan Erdogan, Daniel P. W. Ellis, and John R. Hershey. *Free Universal Sound Separation (FUSS) dataset*, 2020a. https://github.com/google-research/sound-separation/tree/master/datasets/fuss.

Scott Wisdom, Efthymios Tzinis, Hakan Erdogan, Ron J. Weiss, Kevin Wilson, and John R. Hershey. Unsupervised sound separation using mixtures of mixtures. In *Advances in Neural Information Processing Systems*, 2020b.

Yu Wu, Linchao Zhu, Yan Yan, and Yi Yang. Dual attention matching for audio-visual event localization. In *Proceedings of the IEEE International Conference on Computer Vision*, pp. 6292–6300, 2019.

Hang Zhao, Chuang Gan, Andrew Rouditchenko, Carl Vondrick, Josh McDermott, and Antonio Torralba. The sound of pixels. In *Proceedings of the European conference on computer vision (ECCV)*, pp. 570–586, 2018.

A APPENDIX

A.1 QUALITATIVE EXAMPLES

For a range of input SNRs, Figure 4 shows best-case examples of separating on-screen sounds with AudioScope, while Figure 5 shows failure cases. Figures 6 and 7 show random examples at various SNRs, comparing the outputs of semi-supervised SOff 0% models trained with either exact cross entropy (4) or active combinations cross entropy (6). Figure 6 shows the outputs of the two models on 7 random examples, and Figure 7 shows the outputs of the two models on 5 examples that have maximum absolute difference in terms of SI-SNR of the on-screen estimate.

The supplementary material includes audio-visual demos of AudioScope on single mixtures and MoMs with visualizations of MixIT assignments and predicted on-screen probabilities.

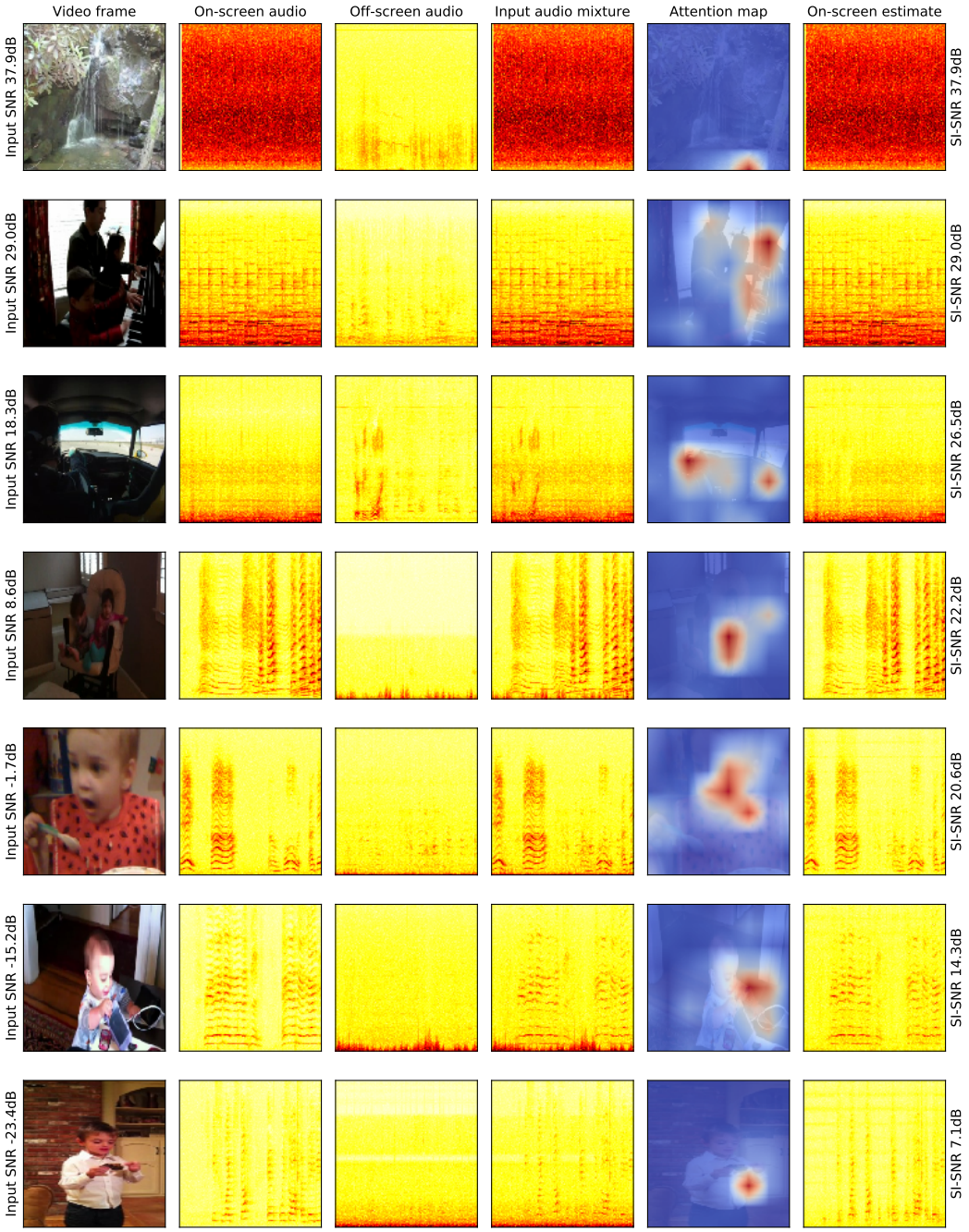

Figure 4: Best cases for AudioScope separation of on-screen sounds under various SNR conditions.

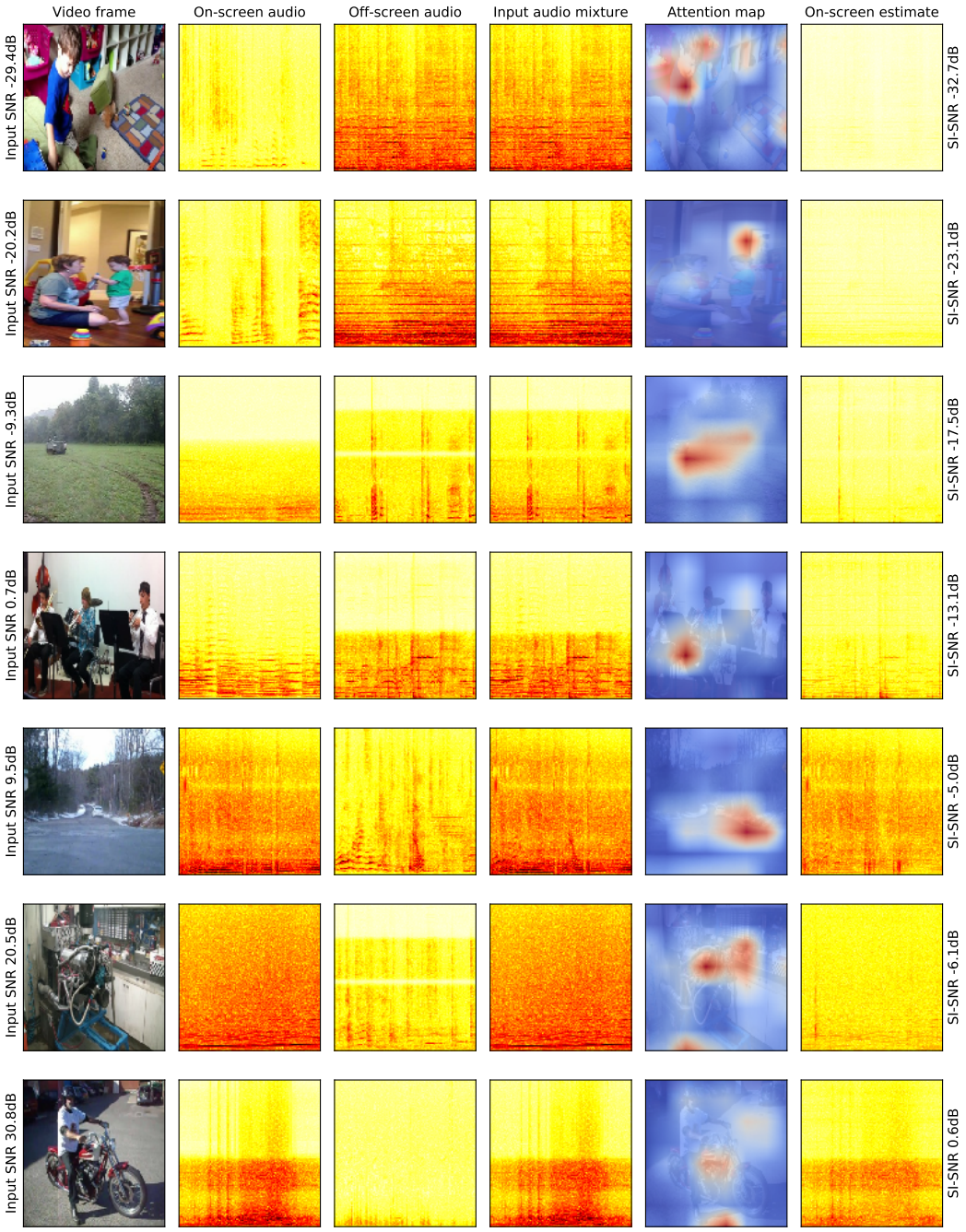

Figure 5: Failure cases for AudioScope separation of on-screen sounds under various SNR conditions.

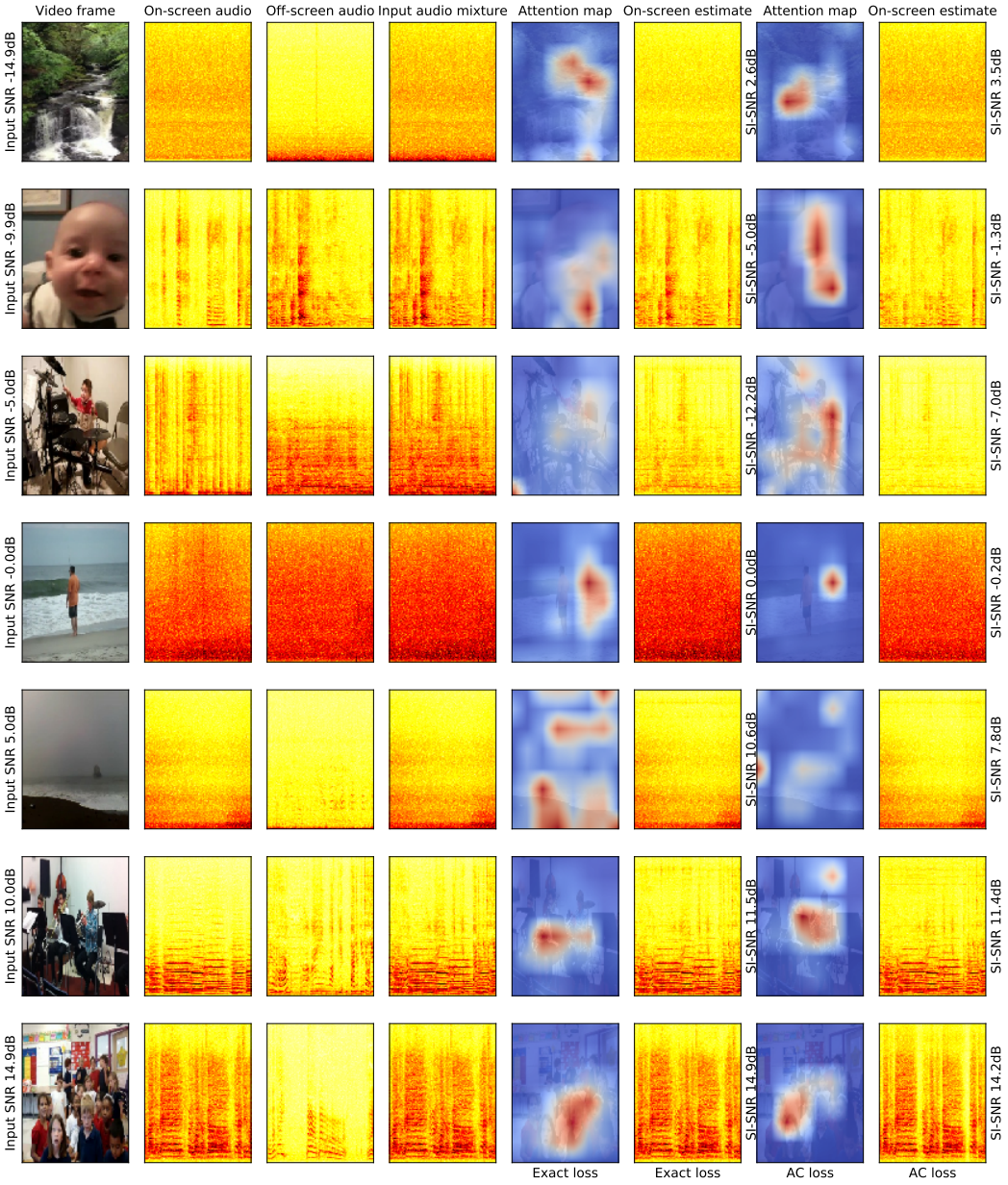

Figure 6: Comparison of random examples of separating on-screen sounds under various SNR conditions using either exact cross entropy (4) or active combinations cross entropy (6) as the classification loss.

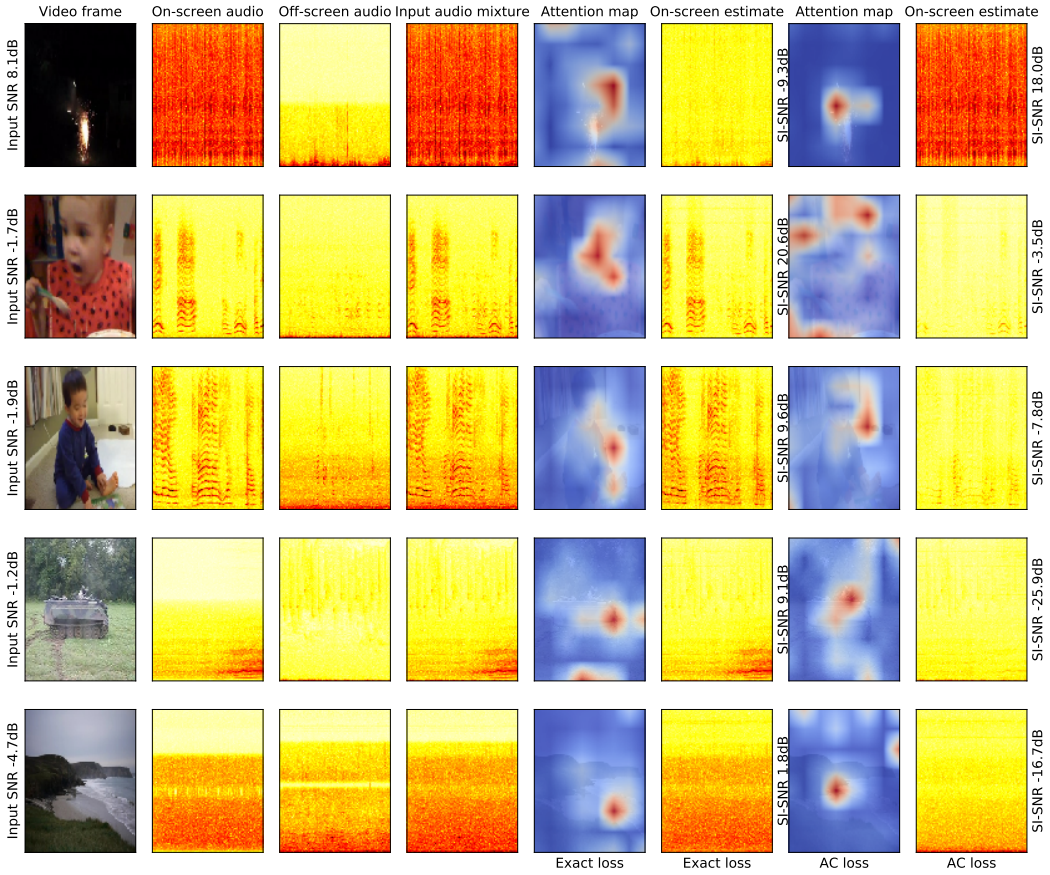

Figure 7: Comparison of examples with maximum absolute performance difference under various SNR conditions using either exact cross entropy (4) or active combinations cross entropy (6) as the classification loss.

A.2 ATTRIBUTIONS

Figure 1
http://www.flickr.com/videos/36499441@N00/9666567231/
Figure 4
http://www.flickr.com/videos/44124419526@N01/3320787733/
http://www.flickr.com/videos/47084925@N00/2609200312/
http://www.flickr.com/videos/95792332@N00/5001149249/
http://www.flickr.com/videos/45746228@N04/5611308670/
http://www.flickr.com/videos/41132143@N00/4731678685/
http://www.flickr.com/videos/31291728@N05/6617479301/
http://www.flickr.com/videos/81295529@N00/8373283856/
Figure 5
http://www.flickr.com/videos/52803775@N08/5956946624/
http://www.flickr.com/videos/94734319@N00/11258800106/
http://www.flickr.com/videos/36766110@N08/8004333249/
http://www.flickr.com/videos/22298070@N00/6816905289/
http://www.flickr.com/videos/47099728@N02/9937024024/
http://www.flickr.com/videos/81295529@N00/9602009921/
Figure 6
http://www.flickr.com/videos/44124419526@N01/4261394492/
http://www.flickr.com/videos/9987082@N04/9116413301/
http://www.flickr.com/videos/94734319@N00/11258737704/
http://www.flickr.com/videos/22298070@N00/4764413052/
http://www.flickr.com/videos/80436976@N00/9550365341/
http://www.flickr.com/videos/19637713@N00/3076521436/
http://www.flickr.com/videos/31255817@N06/3550211268/
Figure 7
http://www.flickr.com/videos/41132143@N00/4731678685/
http://www.flickr.com/videos/52615621@N07/11671932475/
http://www.flickr.com/videos/47099728@N02/9937027064/
http://www.flickr.com/videos/44124419526@N01/2772293317/
http://www.flickr.com/videos/52498883@N05/5337324890/